Novel Formulation for Optimal Schedule with Demand Side Management in Multi-product Air Separation Processes

Shengnan Zhao[1], M. Paz Ochoa[2], Lixin Tang[3,4], Irene Lotero[5], Ajit Gopalakrishnan[5], Ignacio E. Grossmann[2*]*

[1] *Liaoning Engineering Laboratory of Operation Analytics and Optimization for Smart Industry, Northeastern University, Shenyang 110819, China*

[2] *Department of Chemical Engineering, Carnegie Mellon University, Pittsburgh, PA 15213, United States*

[3] *Liaoning Key Laboratory of Manufacturing System and Logistics, Northeastern University, Shenyang 110819, China*

[4] *Institute of Industrial & Systems Engineering, Northeastern University, Shenyang 110819, China*

[5] *Air Liquide, Newark, Newark, DE 19702 United States*

Abstract

In this paper, we address the optimal scheduling of continuous air separation processes with electricity purchased from the day-ahead market, for which we propose a generalized framework to represent different operating states. Specifically, a discrete-time mixed-integer linear programming (MILP) model is developed based on this representation for operating states, which has proven to provide a tight LP relaxation for handling industrial-scale instances. The computational efficiency of the model is demonstrated with data from real industrial production. The response of the scheduling and production level is also tested with various interval lengths for the electricity pricing and length of the time horizon.

1. Introduction

The profitability of energy-intensive process industries is being greatly influenced by the electricity market deregulation that introduces new pricing strategies. Therefore, it is critical for these industries to schedule the production of the plant in order to take advantage of the fluctuations in electricity prices, which is the major part of production costs.

The intelligent management of electricity demand is referred to as demand side management (DSM)[1]. Particularly in the process industry, DSM has recently shown to be a useful tool for industries to efficiently integrate production and energy management. Demand side management technology at the production scheduling and planning level has the advantage of potentially low investment cost, because in general it does not require the purchase of new equipment[2]. It can be categorized as either reducing energy consumption, or rescheduling and shifting energy

demand to off-peak hours. Specifically large-scale, energy intensive processes may play an important role in this context.

In industrial demand side management (iDSM), the electricity supplier provides economic incentives to the industry to modify their electricity consumption by a price-based program and an incentive-based program. In the first one, customers respond to the electricity price structure with voluntary changes in their timing of electricity consumption, taking advantage of low-priced periods and reducing production in high-priced periods. In the latter, customers can obtain electricity at a reduced cost, if the electricity consumption is contracted ahead of time. The consumption curve must then be followed as closely as possible to avoid penalties for over- and under-consumption of electricity[3].

Industrial gases production is an important sector in the chemical industry, and it is a good example of energy-intensive process. Compressor systems consume large amounts of electricity to raise the pressure high enough to achieve cryogenic temperatures for distillation. Due to the recent volatility in energy markets, there is a significant opportunity to reduce costs by taking advantage of lower electricity price periods[4-7]. As shown in many recent works on industrial demand side management (DSM), considering time-sensitive electricity prices can have a significant impact on the load profiles of power-intensive industrial processes. For more details on industrial DSM, a comprehensive literature review can be found in Zhang and Grossmann[1], where air separation works are listed with their main model features.

During the last two decades, a large number of optimization models have been developed to tackle challenging scheduling industrial problems. Floudas and Lin[8], Mendez *et al.*[9], Maravelias [10] and Harjunkoski *et al.*[11] provide detailed reviews of this area. Specifically, there have been several relevant contributions in the area of detailed production scheduling taking into account energy management. Among them, Mitra *et al.* [4] described a discrete-time, deterministic MILP model for optimal production planning of continuous power-intensive processes, emphasizing the systematic modeling of operational transitions with logic constraints. Despite the large size of the MILP models, the required solution times were small due to the effective modeling of transitions. However, only limited number of transitions were taken into account. Subsequently, Mitra *et al.*[12] proposed a generalized model on a component basis that addressed the operational optimization of industrial combined heat and power (CHP) plants. These authors

described the relation between production level and the operating state of units with a linear representation of the projected feasible region. This feasible region was modeled with disjunctions with each term corresponding to linear constraints of a given mode of operation. The linear constraints were generated from offline simulations or from production data. An MILP model was then developed with these constraints and other related to the mass balance and transition modes. Some of the constraints were reformulated with the use of logic, yielding tighter constraints resulting in an improved performance of the model.

Recently, a general discrete-time model was proposed for the scheduling of power-intensive process networks with various power contracts consisting of a network of processes represented by Convex Region Surrogate models that were incorporated in a mode-based scheduling formulation, and allowed modeling a large variety of commonly used power contracts[5]. The resulting MILP model was tested in a real-world industrial test case. Next, Zhang *et al.*[6] developed an integrated stochastic mixed-integer linear programming model considering two sources of uncertainty: spot electricity prices and product demands. In addition, Zhang *et al.*[13] simultaneously optimized long-term electricity procurement and production planning, while considering uncertainty in product demand. They proposed a multiscale multistage stochastic programming MILP model. Recently, Basán *et al.*[7] proposed a novel, efficient and robust formulation, based on a new concept to model the transitions between alternative operating modes called the Process State Transition Network (PSTN). The model was also used to efficiently solve a real-world industrial case study, providing optimal solutions with modest computational effort when considering directed transitions and it only covered the external liquefier of an air separation plant. Another popular representation is the Resource Task Network (RTN), which has been used to provide a generic modeling framework for production scheduling under energy constraints. Castro *et al.*[3,14,15] and Zhang *et al.*[16] proposed scheduling models based on RTN formulations for demand side management.

In order to take into account the dynamic characteristics and performance of the process, some authors have considered its control system at the production scheduling stage. For example, Cao *et al.*[17-19] presented initial results on dynamic modeling and optimization of ASU operations using a large-scale, first principles, detailed dynamic process model. Patisson *et al.*[20] proposed a novel scheduling approach based on scheduling-oriented low-order dynamic models identified from historical process operating data, leading to a dynamic optimization problem aimed

at maximizing profit over the scheduling time horizon. They applied the optimal scheduling method to air separation unit (ASU) producing nitrogen. More recently, Dias *et al*.[21] extended this work by proposing a novel framework for the integration of scheduling and model predictive control (MPC). The framework consisted on identifying scheduling-relevant process variables, building low-order dynamic models to capture their evolution, and integrating scheduling and MPC. They achieved significant cost reductions with reasonable computational times when applying the methodology to an ASU.

Apart from the air separation industry, demand side management has been applied to other energy intensive processes. Nolde and Morari[22] presented a continuous time scheduling model that was successfully applied for the electrical load tracking scheduling of a steel plan. The formulation uses six different binary variables to capture the relation of a production task to its placement within a grid of uniform time intervals. An improvement was proposed by Hait and Artigues[23] resulting in fewer constraints and binary variables. The same approach was adopted by Hadera *et al*.[2], where they addressed the scheduling of the melt shop section of a stainless steel production plant using a two-binary variable concept instead of six-binary variable concept, and extended the formulation to account for multiple purchase contracts. Recently, Hadera *et al*.[24] presented an improvement concerning the modeling of the coupling between the scheduling problem and the computation of the energy bill. Castro *et al*.[25] applied Nolde and Morari's concept of the six cases of task-time interval relations to optimize the maintenance of a gas-fired power plant. Using Generalized Disjunctive Programming, the authors found a tighter formulation that considers the electricity consumption. Later, Zhao *et al*.[26] applied and modified the GDP constraints in Castro *et al*.[25] to a continuous time MILP model with variable number of time slots for the scheduling problem of steel production. A brief overview of enterprise-wide optimization, and challenges in multiscale temporal modeling and integration of different models for planning, scheduling and control is presented in Castro *et al*.[27], where GDP is reviewed and illustrated with the STN and RTN representations.

As one of the major challenges in the area of scheduling is to effectively solve large-scale models[27], the main contribution of this paper is the following. We propose a new representation to handle operating states and transitions, and formulate the corresponding mixed-integer linear programming model whose LP relaxation is tight, making it suitable for industrial applications. Specifically, we consider air separation processes that involve multiple units and

multiple products. The framework is flexible and can be applied not only to air separation production, but also other continuous processes with similar production features.

The remaining paper is organized as follows. In section 2, a brief description of air separation production and electricity pricing strategy are presented to help understand the scheduling problem. In Section 3, we present the problem statement of optimal scheduling with demand side management for air separation production. In section 4, the Advanced Process State Transition Network (APSTN) is proposed to represent the scheduling problem addressed in this paper. Applying the new framework previously presented in section 4, an MILP model is developed in section 5 in which some constraints are reformulated as tighter formulations in section 6. In section 7, two alternative formulations of similar problems are presented and compared to our model in section 8. Finally, the conclusions of this paper are discussed in section 9.

2. Background

Air separation process

The air is approximately composed of 78% nitrogen, 21% oxygen and 0.9% argon. The purified components of air are raw materials for many manufacturing processes. Oxygen is widely used among different industries, such as metal manufacturing mainly for steel production; chemical, pharmaceutical and petroleum use it in many oxidation processes; glass and ceramic industry; pulp and paper manufacturing; health care uses; etc. Moreover, gaseous nitrogen is commonly used as an inert replacement for air in several industries.

The main task of air separation production is to separate its components by cryogenic distillation conducted in Air Separation Units (ASUs)[20]. As shown in Figure 1, an ASU generally consists of an air compressor system and a rectifying unit. The production process can be described as follows. The air at ambient temperature is compressed by a main air compressor. After removing air impurities in the front-end-purification systems, the compressed air is either sold directly or sent to rectifying units, where various liquid products and gas products are separated from the liquefied air according to their different boiling points.

The production of air separation is a continuous process, where the production levels are achieved by properly adjusting the operation of the ASUs to meet various production constraints, mainly to satisfy the different product demands and inventory levels. This can be interpreted as the transition of operation states of the production system.

It is important to note that there is a correlation of the production level between the different liquid products during the production.

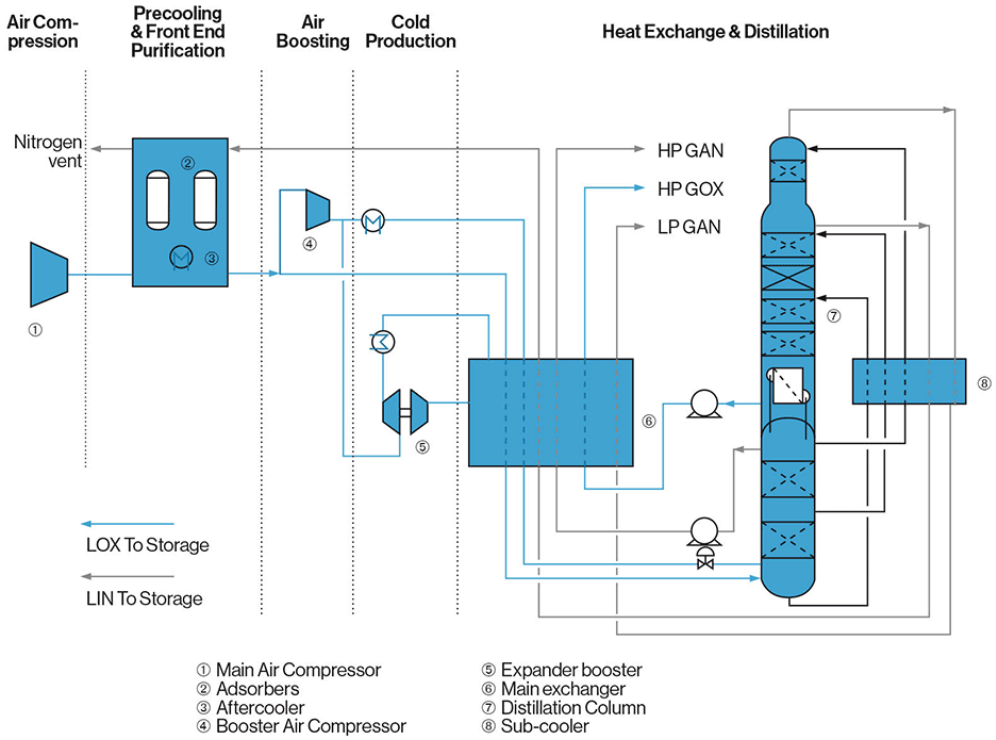

Figure 1. Typical Large ASU arrangement (https://www.engineering-airliquide.com/large-air-separation-unit)

Electricity market

The available amount of electrical energy and the electricity price are defined by purchasing contracts, including: (i) long-term contract (base contract or base load) with constant price and constant amount of electricity delivered over time; (ii) short-term contract (Time-of-Use or TOU) with two price levels (on-and off-peak); (ii) spot market (day-ahead) where prices vary hourly, assumed to be known 24 h ahead; and (iv) onsite generation with constant price with additional start-up costs.

In this paper, we assume that the electricity is purchased from the day-ahead market, which lies inside the category of spot market. In this market, power produced by all generators is pooled on its way to the consumers creating a desirable economy of scale. The auction-based trading is managed by the independent system operator (ISO). First, power generation companies submit their bids, and then consumers submit their offers. The market is cleared at the price where the supply and demand curves intersect. All generators with bid prices below or at the

clearing price have to provide the amount of power corresponding to their accepted bids, and all consumers with offer prices above or at the clearing price are allowed to draw the corresponding amount of energy from the system[1]. Different markets are cleared at different frequencies. For example, the day-ahead market is cleared once every day. Therefore, the price follows regional fluctuations of electricity availability varying on an hourly basis. The exact prices of the day-ahead contract depend on the market the plant enters and contractual commitments with the local operator.

3. Problem statement

In this paper, we consider the production of an air separation plant, which produces various liquid products including liquid nitrogen (LIN), liquid oxygen (LOX) and liquid argon (LAR), as well as gaseous products, including high-pressure gaseous oxygen (HPGOX) and compressed air (CA). The production is performed at parallel heterogeneous ASUs. The site has operational flexibility. Production is modulated by adjusting the operating state of the units to meet customer demand at the lowest cost. Gaseous products are delivered directly to customers through pipelines, while liquid products can be stored in tanks at the site. The electricity is assumed to be purchased from the day-ahead market. This market is cleared the day before the energy is consumed, so prices are known one day in advance. It is assumed that there is an electricity price forecast available for the remaining days of the week (D+2 to D+7).

In general, the operating states are characterized by the following features:

1) Some specific operating states have corresponding minimum operating time before transitioning to another state, imposed by operability and equipment requirements;

2) There are pre-defined directions for several state transitions. In other words, the transitions can only occur from the current state to a set of specified states;

3) There are start-up costs of some specific state transitions. As already mentioned, the large-scale equipment of air separation production is mainly driven by electricity. When turning on or shutting down equipment, there are significant costs that are involved. Normally, frequent on-off transitions should be avoided. However, the optimal schedule of operating states may be influenced by the fluctuation of electricity prices. The start-up cost is therefore considered in the objective of the scheduling problem.

The goal of the scheduling problem is to select the operating point for each of the ASUs to minimize the total production costs that include electricity consumption, transition between operating states and backup of products, while satisfying the different product demands. The following information is assumed to be given:

- The length of the scheduling time horizon
- The set of ASUs with different configurations
- The set of products to be produced, including liquid products {LOX, LIN, LAR} and gaseous products {HPGOX, CA}
- A set of operating states of each ASU and the parameters that defined the operation state
- The initial inventory of liquid products, feasible inventory levels during production, and final inventory levels by the end of the production horizon
- The demand of products on an hourly basis
- The forecast of electricity prices within the scheduling time horizon
- The fixed cost of each allowed state transition

In order to optimize the production of air separation, the following decisions are made for each time period:

- The operating state for each ASU
- The load of each plant (i.e. the air flow through the main air compressors)
- The production level of each product
- The transition of operating states

4. New Representation: Advanced Process State Transition Network

In order to address the scheduling problem, the continuous operating region of the air separation process is discretized into several operating states according to the production tasks. Generally, the tasks to be scheduled in a sequential environment can be represented by either precedence based or time-grid-based models[11]. Known for being concise and easy to implement, the precedence based representation is widely used, especially when accounting for setups between tasks. Time-grid-based representations tend to be tighter and computationally superior than the precedence based representation, despite generating larger models that are less intuitive[11]. Especially for air separation process, a new framework, namely process state transition network (PSTN), was recently proposed by

Basán *et al.*[7] to address the scheduling of nitrogen production in an external liquefier, whose basis is a time-grid-based representation.

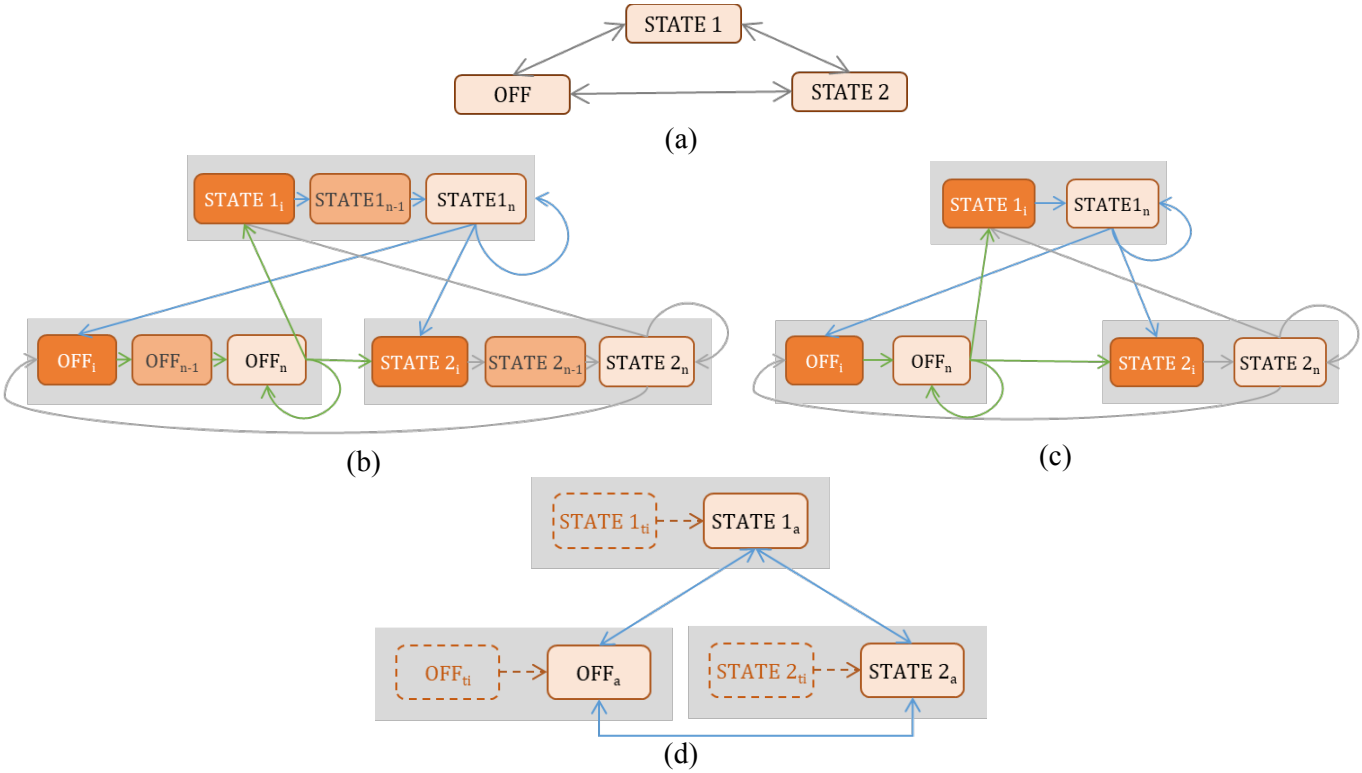

Figure 2. Description of the evolution of the PSTN (a) Operation described by three states with minimum operating time; (b) PSTN representation, and (c) modified PSTN representation where the sub-indices *i*, *n-1* and *n* stand for initial, intermediate and final sub-states, respectively. (d) APSTN representation, where sub-indices *ti* and *a* stand for transition indicator and actual.

The basic idea of PSTN is to disaggregate the states that have minimum operating time into three sub-states: initial sub-state, intermediate sub-state and final sub-state. An illustrative example can be found in Fig 2. With the disaggregated sub-states, the whole transition network (Fig. 2(a)) is represented as a directed graph, as can be seen in Fig. 2(b). This framework for representing the transitions is especially efficient when many of the transitions are restricted, and there is a limited number of states with minimum operating time.

In this paper, we propose an extension of the PSTN, namely the Advanced PSTN (APSTN). We first notice that the intermediate sub-state of the PSTN can be eliminated by considering that the plant has to operate one hour in the

initial state and the minimum operating time minus one hour in the final state as shown in Fig. 2 (c). This first modification results in a 30% reduction of the number of binary variables.

Based on the concept of the PSTN, we now disaggregate the states with minimum operating time into two items: transition indicator sub-states and actual sub-states. The objective of the transition indicator sub-state is merely to point out if there is a transition between the different states, in order to account for the minimum operating time once the transition is detected. With this objective in mind, we only relate the state transitions constraints (details in Section 5) to this indicator. As a result, the number of constraints is significantly reduced. On the other hand, the actual sub-states are involved in all model constraints: the state transition constraints and the production constraints. The actual sub-states are linked to each other as shown in Fig. 2 (d), as the transition indicator sub-state is considered as a "dummy" state that only registers transitions.

In summary, we use the concept of state disaggregation introduced in the PSTN to account for the minimum operating time without introducing a new index for the states in the binary variable. Instead of considering a sequential disaggregation (initial, intermediate and final sub-states), we consider a parallel disaggregation (transition indicator and actual sub-states).

To illustrate the different formulations, we consider the transition from the shutdown state OFF to a state S1, with minimum operating time of 5 hours, and then the transition from state S1 to state OFF. As can be seen in Figure 3, the PSTN consists of a three sub-state partition: the initial sub-state of S1 at t=3h, the intermediate sub-state of S1 at t=4h and the final sub-states of S1 from t=5h to t=7h, where all model constraints stand for every sub-state. On the other hand, there are only two sub-states in the modified PSTN: initial sub-state at t=3h and final sub-states from t=4h to t=7h. Finally, in the APSTN two sub-states can also be distinguished: the transition indicator at time t=3h, where the state transition takes place, and the actual sub-state accounting from t=3h to t=7h. In this representation, the transition indicator sub-state is regarded as "dummy sub-state" because its purpose is only to indicate if there is any transition. Therefore, it is only considered in the state transitions constraints, whereas the actual sub-state is considered in both state transition and production constraints.

Therefore, the two major differences between the PSTN and APSTN representations can be summarized as follows: (i) The elimination of the intermediate sub-state, resulting in a reduction of one third of the number of binary

variables; and (ii) the reduction of the number of constraints in two ways. First, the transition indicator sub-states are not counted in the production related constraints, such as constraints (1)-(18) described in Section 5; second, since the intermediate operating state of PSTN is eliminated, the constraints that are related to intermediates sub-state are consequently eliminated in the APSTN model, which also yields reductions in the number of constraints.

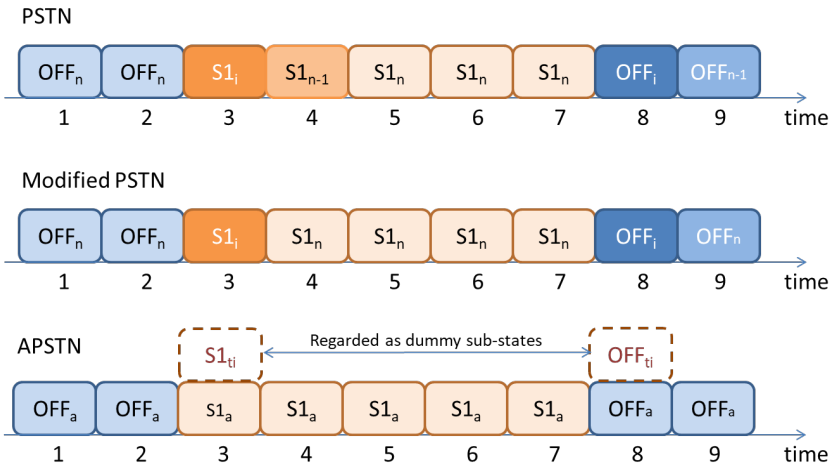

Figure 3. Different state partition for the PSTN, modified PSTN and APTSN formulations. Subscripts *i*, *n-1*, *n*, *ti*, and *a* stand for initial, intermediate, final, transition indicator, and actual, respectively.

5. Mathematical Formulation

Nomenclature Section

Indices

c	Unit
s, s', ss, ss'	Operation state
i	Liquid product
t	Time interval

Sets

C	The set of units C={$c1$,$c2$}
S_c	The set of real production states for unit c, $S_c = S_c^a \cup NS_c$
S_c^a	The set of actual sub-states for unit c
$S_{c,s}^i$	The set of transition indicator sub-states corresponding to unit c and actual sub-state s
$FS_{c,s}$	The set of states from which are forbidden to transit to state s of unit c
$TO_{c,s}$	The set of states from which are allowed to transit to state s of unit c

NS_c	The set of states not having minimum operating time
I	The set of liquid products I= {LOX, LIN, LAR}
T	The set of time periods in the scheduling time horizon T={1, 2,…,TL}

Parameters

$\alpha 1_{c,s}, \beta 1_{c,s}$	Correlation parameters for compressed air, regarding to state s of unit c
$\alpha 2_{c,s}, \beta 2_{c,s}$	Correlation parameters for turbine, regarding to state s of unit c
$\alpha 3_{c,s}, \beta 3_{c,s}, \gamma_{c,s}$	Correlation parameters of electricity consumption and air inlet to unit, air inlet to turbine and constant consumption
$QA_{c,s}^{min}, QA_{c,s}^{max}$	Minimum and maximum amount of air inlet to unit, regarding to state s of unit c
$QCA_{c,s}^{min}, QCA_{c,s}^{max}$	Minimum and maximum amount of compressed air to customers, regarding to state s of unit c
$QT_{c,s}^{min}, QT_{c,s}^{max}$	Minimum and maximum amount of air inlet to turbine, regarding to state s of unit c
$QL_{c,s,i}^{min}, QL_{c,s,i}^{max}$	Minimum and maximum production level of liquid product i, regarding to state s of unit c
$QG_{c,s}^{min}, QG_{c,s}^{max}$	Minimum and maximum production level of HPGOX, regarding to state s of unit c
D_t^{Air}	The demand of compressed air at time t
D_t^G	The demand of HPGOX at time t
$D_{i,t}^L$	The demand of liquid i at time t
$Init\ Inv_i$	Initial inventory of liquid product i
Inv_i^{min}, Inv_i^{max}	The minimum and maximum amount of inventory of liquid product i
$FinalInv_i^{min}, FinalInv_i^{max}$	The minimum and maximum amount of final inventory of liquid product i
$P_{c,s}^{min}, P_{c,s}^{max}$	The minimum and maximum amount of available electricity, regarding to state s of unit c
$cost\ EP_t$	The electricity price of time t
$cost\ QBK$	The cost of backup oxygen
$cost\ Tr_{c,s,s'}$	Transition cost from state s to state s' of unit c
ms_s	The minimum consecutive operating time of state s
$M_c^{QA}, M_{c,s}^{QACorr}$	Sufficient large number for air inflow related constraints (Eq. (1), Eq.(2)), regarding to c and s
M_c^{QCA}	Sufficient large number for compressed ????related constraint Eq. (3)
M_c^{QT}	Sufficient large number for air to turbine related constraint Eq.(5)
$M_{c,s}^{LOX\_UB}, M_{c,s}^{LOX\_LB}$	Upper and lower bound for LOX correlation
$M_{c,s}^{LAR\_UB}, M_{c,s}^{LAR\_LB}$	Upper and lower bound for LAR correlation
$M_{c,i}^{QL}$	Sufficient large number of liquid production constraint Eq.(8)
M_c^{QG}	Sufficient large number of HPGOX production constraint Eq. (9)
M_c^P	Sufficient large number of power consumption constraint Eq.(18)

Binary variables

$y_{c,s,t}$	Equals to 1 if unit *c* is operated at *s* state during time *t*
Continuous variables	
$QA_{c,t}$	Inlet flowrate of Air to unit *c* during time *t*
$QT_{c,t}$	Inlet flowrate of Air to turbine from unit *c*
$QL_{c,i,t}$	Liquid component *i* production in unit *c* during time *t*
$QG_{c,t}$	High pressure gaseous oxygen production in unit *c* during time *t*
$QCA_{c,t}$	Compressed air production in column *c* during time *t* to costumers
QBK_t	Backup oxygen during time *t*
$P_{c,t}$	Total power consumption by column *c* during time *t*
TC	Total production costs

Using the APSTN representation as the basis, we formulate the MILP model for the scheduling problem addressed in this paper. The formulation is based on discrete time representation, where the time horizon *T* is divided into time intervals *t* of equal length, over which the electricity pricing is given. The continuous variables in the model are restricted to be positive. The notation of indices, sets, parameters and variables can be found in the Nomenclature section. The mathematical formulation is presented below.

5.1 Capacity constraints

The capacity constraints restrict the air flow in the ASU. The relationship of air inflow to unit *c* at time *t*, $QA_{c,t}$, and the compressed air to costumers, $QCA_{c,t}$, that is produced in unit *c* during time *t* is represented by constraint (1), where *C* is the set of units, S_c is the set of operating states that are related to unit *c,* and $\beta 1_{c,s}$ is the fixed volume of air that needs to be delivered to the unit *c* when *c* is operating in state *s*.

$$QA_{c,t} \leq \alpha 1_{c,s} \cdot QCA_{c,t} + \beta 1_{c,s} \cdot y_{c,s,t} + M_{c,s}^{QACorr} \cdot (1 - y_{c,s,t}), \forall c \in C, s \in S_c, t \in T \quad (1)$$

The amount of the air inflow is restricted by the unit capacity, described by constraint (2). The maximum and minimum flow rate parameters in the model, such as $QA_{c,s}^{min}$ and $QA_{c,s}^{max}$ in constraint (2), correspond to the unit *c* and state *s*. When the unit c is operated with state *s* at time *t*, e.g. $y_{c,s,t} = 1$, then the bounding constraint is activated, where $QA_{c,t}$ varies between the minimum and maximum flow-rate; otherwise, the constraint is relaxed. It is important to note that the values of the parameter M in this paper are selected with respect to the bounding values of

the variables in the constraints. Therefore, we use different values of parameter M in different constraints, in order to obtain a better LP relaxation of the model. Besides, other representation of bounding constraints has been tried, e.g. generalized disjunctive programming and the hull reformulation. However, there is no obvious improvement of the model performance in this case.

Likewise, the maximum and minimum amount of compressed air to customer is represented in constraint (3).

$$QA_{c,s}^{min} \cdot y_{c,s,t} \leq QA_{c,t} \leq QA_{c,s}^{max} + M_c^{QA} \cdot (1 - y_{c,s,t}), \forall c \in C, s \in S_c, t \in T \quad (2)$$

$$QCA_{c,s}^{min} \cdot y_{c,s,t} \leq QCA_{c,t} \leq QCA_{c,s}^{max} + M_c^{QCA} \cdot (1 - y_{c,s,t}), \forall c \in C, s \in S_c, t \in T \quad (3)$$

As shown in Fig.4, there is a turbine in unit 2 to increase the liquid production out of distillation column. Regarding the turbine, the correlation of the total air inflow to unit $QA_{c,t}$ and the air inflow to turbine $QT_{c,t}$ is represented by constraint (4). Constraint (5) represents the upper and lower bounds of $QT_{c,t}$.

$$QT_{c,t} \leq \alpha 2_{c,s} \cdot QA_{c,t} + \beta 2_{c,s} \cdot y_{c,s,t}, \forall c = c2, s \in S_c, t \in T \quad (4)$$

$$QT_{c,s}^{min} \cdot y_{c,s,t} \leq QT_{c,t} \leq QT_{c,s}^{max} + M_c^{QT} \cdot (1 - y_{c,s,t}), \forall c = c2, s \in S_c, t \in T \quad (5)$$

5.2 Production level constraints

Due to confidentiality reasons, the explicit formulations of part of the models are not given below but only the general forms of the constraints are shown. The correlation of different liquid products during the production is formulated with inequalities. As represented by constraints (6), the production amount of LOX is subject to an affine function of the operating state and associated air inflow to unit, air inflow to turbine (if there is one) and production of LIN and HPGOX. Similarly, the affine inequalities (7) describe the correlations associated with the production of LAR.

$$QL_{c,LOX,t} \leq f(QA_{c,t}, QT_{c,t}, QG_{c,t}, QL_{c,LIN,t}, y_{c,s,t}) + M_{c,s}^{LOX\_UB} \cdot (1 - y_{c,s,t}), \forall c \in C, s \in S_c, t \in T \quad (6a)$$

$$QL_{c,LOX,t} \geq f(QA_{c,t}, QT_{c,t}, QG_{c,t}, QL_{c,LIN,t}, y_{c,s,t}) - M_{c,s}^{LOX\_LB} \cdot (1 - y_{c,s,t}), \forall c \in C, s \in S_c, t \in T \quad (6b)$$

$$QL_{c,LAR,t} \leq g(QA_{c,t}, QG_{c,t}, QL_{c,LIN,t}, y_{c,s,t}) + M_{c,s}^{LAR\_UB} \cdot (1 - y_{c,s,t}), \forall c \in C, s \in S_c, t \in T \quad (7a)$$

$$QL_{c,LAR,t} \geq g(QA_{c,t}, QG_{c,t}, QL_{c,LIN,t}, y_{c,s,t}) - M_{c,s}^{LAR\_LB} \cdot (1 - y_{c,s,t}), \forall c \in C, s \in S_c, t \in T \quad (7b)$$

Following are the boundary constraints for various products. The production level of each product is restricted to vary within a feasible range given by constraints (8)-(9).

$$QL_{c,s,i}^{min} \cdot y_{c,s,t} \leq QL_{c,i,t} \leq QL_{c,s,i}^{max} + M_{c,i}^{QL} \cdot (1 - y_{c,s,t}), \forall c \in C, s \in S_c, i \in I, t \in T \quad (8)$$

$$QG_{c,s}^{min} \cdot y_{c,s,t} \leq QG_{c,t} \leq QG_{c,s}^{max} + M_{c}^{QG} \cdot (1 - y_{c,s,t}), \forall c \in C, s \in S_c, t \in T \quad (9)$$

The oxygen balance of the production in the units can be formulated as affine inequalities as represented with constraints (10).

$$h(QA_{c,t}, QT_{c,t}, QL_{c,LOX,t}, QG_{c,t}, y_{c,s,t}) \geq 0, \forall c \in C, s \in S_c, t \in T \quad (10)$$

5.3 Demand constraints

The production of gaseous products, which are CA and HPGOX, are subject to the demand requirements regarding to each time period, as represented by constraints (11) and (12), respectively. As for liquid products, since they are temporally stored in tanks and delivered to customers periodically, the related demand constraint is given through the inventory level constraints in the following section.

$$\sum_{c} QCA_{c,t} \geq D_t^{Air}, \forall c \in C, t \in T \quad (11)$$

$$\sum_{c} QG_{c,t} + QBK_t \geq D_t^{HPG}, \forall c \in C, t \in T \quad (12)$$

5.4 Inventory level constraints

As mentioned before, the liquid products are delivered to customers periodically via trucks and trailers. The surplus of a product is stored in tanks, which leads to the constraints for inventory levels. For each product, the amount of cumulative production over a time period plus the initial inventory and minus the demand, has to lie within the feasible range of inventory level, as represented by constraints (13)-(14). The inequality for the inventory constraint of LOX in (14) is distinguished from (13), for other liquid products, because LOX can be vaporized and used as backup to supply the gas customer. By the end of the time horizon, the inventory level is subject to final inventory requirements, as shown with (15)-(16).

$$Inv_i^{min} \leq InitInv_i + \sum_{c \in C} \sum_{tt \leq t} QL_{c,i,tt} - \sum_{tt \leq t} D_{i,tt}^{L} \leq Inv_i^{max}, \forall i \in I \backslash \{LOX\}, t \in T \quad (13)$$

$$Inv_{LOX}^{min} \leq InitInv_i + \sum_{c \in C} \sum_{tt \leq t} QL_{c,i,tt} - \sum_{tt \leq t} D_{i,tt}^{L} - \sum_{tt \leq t} QBK_{tt} \leq Inv_i^{max}, \forall i = LOX, t \in T \quad (14)$$

$$FinalInv_i^{min} \leq InitInv_i + \sum_{c\in C}\sum_{t\leq T} QL_{c,i,t} - \sum_{t\leq T} D_{i,t}^{L} \leq FinalInv_i^{max}, \forall i \in I\backslash\{LOX\} \quad (15)$$

$$FinalInv_i^{min} \leq InitInv_i + \sum_{c\in C}\sum_{t\leq T} QL_{c,i,t} - \sum_{t\leq T} D_{i,t}^{L} - \sum_{t\leq T} QBK_t \leq FinalInv_i^{max}, \forall i = LOX \quad (16)$$

5.5 Energy consumption calculation

The electricity consumption $P_{c,t}$ is the sum of the power consumed by the main air compressors according to the operating state of the equipment. The calculation of electricity consumption is represented by constraints (17). This is a general formulation, which can be extended to any operation states. With respect to the case study in this paper, the inequality (17) is reformulated as equation (29), detailed in section 6, by removing the big-M.

$$P_{c,t} \geq \alpha 3_{c,s} \cdot QA_{c,t} + \beta 3_{c,s} \cdot QCA_{c,t} + \gamma_{c,s} \cdot y_{c,s,t} - M \cdot (1 - y_{c,s,t}), \forall c \in C, s \in S_c, i \in I, t \in T \quad (17)$$

Constraint (18) restricts the availability of electricity consumption.

$$P_{c,s}^{min} \cdot y_{c,s,t} \leq P_{c,t} \leq P_{c,s}^{max} + M_c^P \cdot \left(1 - y_{c,s,t}\right), \forall c \in C, s \in S_s, i \in I, t \in T \quad (18)$$

5.6 State transitions constraints

In this section, the constraints related to the APSTN framework are presented. Logic constraints are developed to condition the transitions between operating states. As mentioned before, the transition indicator sub-state and actual sub-state are two different states: Transition indicator sub-states are dummy states, which indicate when a transition occurs, while the actual sub-states are real production states. As stated in equation (19), for each time period *t*, the unit *c* can only be in one of the production states $s \in S_c$, where $S_c = NS_c \cup S_c^a, NS_c$ is the set of states that are not disaggregated and S_c^a is the set of actual sub-states corresponding to *c*.

$$\sum_{s\in S_c} y_{c,s,t} = 1 \quad , \forall c \in C, t \in T \quad (19)$$

The state pair $(s, s'), s \in S_{c,s'}^i, s' \in S_c^a$ in constraints (20)-(23) and (26) refers to the associated transition indicator and actual sub-states regarding unit *c*, where $s \in S_{c,s'}^i$ is the transition indicator sub-state linked to actual sub-state *s'*. If a transition indicator sub-state *s* is activated at time *t*, then the corresponding actual sub-state *s'* will be activated in the same time period *t*, as shown by constraint (20).

$$y_{c,s,t} \le y_{c,s',t}, \forall c \in C, t \in T, s \in S^i_{c,s'}, s' \in S^a_c \quad (20)$$

As stated by (21), if an actual sub-state *s'* is active in time period *t*+1, then there are only two possibilities: either *s'* is also active in previous time period *t*, or there is a transition occurring from other state to state *s'* in time *t*+1.

$$y_{c,s',t+1} \le y_{c,s,t+1} + y_{c,s',t}, \forall c \in C, t \in T, s \in S^i_{c,s'}, s' \in S^a_c \quad (21)$$

Constraint (22) defines a state transition that occurs at time *t,* when *t*-1 and *t* are operated in different states. $TO_{c,s'}$ is the set of states from which are allowed to transit to state *s'* of unit *c*.

$$y_{c,s,t} \ge y_{c,s',t} + \sum_{ss \in TO_{c,s'}} y_{c,ss,t-1} - 1, \forall c \in C, t \in T, s \in S^i_{c,s'}, s' \in S^a_c \quad (22)$$

Constraint (23) states that if the transition indicator sub-state is activated at time *t*, then it implies that the associated actual sub-state should not be operated at time *t-1*.

$$y_{c,s,t} + y_{c,s',t-1} \le 1, \forall c \in C, t \in T, s \in S^i_{c,s'}, s' \in S^a_c \quad (23)$$

Equation (24) represent that at most one state transition occurs in each time period *t*.

$$\sum_{s \in S^i_c} y_{c,s,t} \le 1, \forall c \in C, t \in T \quad (24)$$

Since the APSTN has some predefined sequence of operation states, the state transition cannot occur between arbitrary two states. Constraint (25) guarantees that forbidden transitions will not occur. $FS_{c,s}$ is the set of states from which are forbidden to transit to state *s* of unit *c*.

$$y_{c,s,t} + y_{c,s',t-1} + y_{c,ss,t} + y_{c,ss',t-1} \le 1, \forall c \in C, t \in T, s \in S^i_{c,s'}, s' \in S^a_c, ss \in FS_{c,s}, ss' \in S^i_{c,ss} \quad (25)$$

Constraint (26) requires that when the actual state *s'* is first operated, it has to be operated consecutively for $ms_{s'}$ time intervals. $ms_{s'}$ is the minimum operating time of state *s'*.

$$y_{c,s',t} \ge \sum_{k=0}^{ms_{s'}-1} y_{c,s,t-k}, \forall c \in C, t \in T, s \in S^i_{c,s'}, s' \in S^a_c \quad (26)$$

In order to account for the transition costs, the logic proposition $Y_{c,s,t} \wedge Y_{c,s',t+1} \Rightarrow TR_{c,t+1} = cost\, Tr_{c,s,s'}$ represents the transition costs between operating states: if there is transition from state *s* to state *s*' at time *t*+1, then the transition cost $TR_{c,t+1} = cost\, Tr_{c,s,s'}$; otherwise $TR_{c,t+1}$ is equal to zero. This logic proposition is

formulated with constraint (27), which is reformulated to tighter formulations in section 6.2 with a set of constraints by introducing auxiliary continuous variables.

$$TR_{c,t+1} \geq cost\,Tr_{c,s,s'} \cdot (y_{c,s,t} + y_{c,s',t+1} - 1), \forall c \in C, t \in T \backslash \{TL\}, s' \in S_c, s \in TO_{c,s'}\, cost\,Tr_{c,s,s'} \neq 0 \quad (27)$$

It is important to note that the transition indicator sub-states are only involved in the state transition constraints. The reason for applying this modeling strategy is as follows. In the addressed scheduling problem, we consider a relatively detailed level of production, and therefore, the proposed model involves many production constraints. Considering that the sub-states are the replications of their aggregated states, which means the sub-states share the same production features, it is enough to choose either the transition indicator sub-state or the actual sub-state involved in the production related constraints. By applying this constraint reduction strategy, the model becomes more compact and the solution time can be reduced significantly, which will be demonstrated in section 8.

5.7 Objective function

The objective function given by (28) minimizes the total production costs *TC*, including power consumption cost, state transition cost and cost of oxygen backup. The transition cost is essentially the cost of additional electricity consumption during transition periods. $cost\,EP_t$ is the electricity price forecast in time *t*.

$$TC = \sum_{c \in C} \sum_{t \in T} cost\,EP_t \cdot (P_{c,t} + TR_{c,t}) + \sum_{t \in T} cost\,QBK \cdot QBK_t \quad (28)$$

In summary, the original MILP model is given by minimizing objective in (28) subject to constraints (1) – (27). However, we can actually improve the formulations by reformulating some of the constraints to get a tighter LP relaxation of the model, as will be shown in the next section.

6. Constraint reformulation

6.1 Reformulation of power consumption constraint

As formulated with (17), except for a state dependent fixed cost $\gamma_{c,s}$, the power consumption $P_{c,t}$ is also dependent on the amount of air inflow $QA_{c,t}$ and compressed air $QCA_{c,t}$. Analyzing the cases of industrial application, an observation is that when the ASUs are set in shutdown states, the fixed cost $\gamma_{c,s}$, the air inflow $QA_{c,t}$ and the compressed air $QCA_{c,t}$ all equal to zero. Consequentially, the power consumption of shutdown states should be zero, which implies that $P_{c,t}$ only need to account for the production states. By excluding the shutdown state, we

are able to reformulate (17) as constraint (29), where the big-M is removed. The tightness of LP relaxation of the formulations with big-M constraints greatly depends on the value of the big-M. In addition, the power consumption $P_{c,t}$ is an important term of the objective functions in this paper. Therefore, the performance of the model is significantly improved with constraint (29).

$$P_{c,t} \geq \alpha 3_{c,s} \cdot QA_{c,t} + \beta 3_{c,s} \cdot QCA_{c,t} + \gamma_{c,s} \cdot y_{c,s,t}, \forall c \in C, s \in S_c \backslash \{ShutDown\}, i \in I, t \in T \quad (29)$$

6.2 Reformulation of transition cost constraint

Constraint (27) is the most common way to interpret the logical proposition $Y_{c,s,t} \wedge Y_{c,s',t+1} \Rightarrow TR_{c,t+1} = cost\,Tr_{c,s,s'}$. Here, we develop another formulation corresponding to the logical proposition accounting for the transition costs, which is represented with equation (30).

$$TR_{c,t+1} = cost\,Tr_{c,s,s'} \cdot y_{c,s,t} \cdot y_{c,s',t+1}, \forall c \in C, t \in T \backslash \{TL\}, s' \in S_c, s \in TO_{c,s'}, cost\,Tr_{c,s,s'} \neq 0 \quad (30)$$

The bi-linear terms of the binary variables in (30) are linearized by applying the exact linearization strategy, proposed by Glover[28]. Let $x_{c,s,s',t+1} = y_{c,s,t} \cdot y_{c,s',t+1}$, where $x_{c,s,s',t}$is a continuous variable with range of [0,1], then the equation in (30) can be rewritten as the following set of constraints:

$$TR_{c,t+1} = cost\,Tr_{c,s,s'} \cdot x_{c,s,s',t+1}, \forall c \in C, t \in T \backslash \{TL\}, s' \in S_c, s \in TO_{c,s'}, cost\,Tr_{c,s,s'} \neq 0 \quad (31)$$

$$x_{c,s,s',t+1} \geq y_{c,s,t} + y_{c,s',t+1} - 1, \forall c \in C, t \in T \backslash \{TL\}, s' \in S_c, s \in TO_{c,s'}, cost\,Tr_{c,s,s'} \neq 0 \quad (32)$$

$$x_{c,s,s',t+1} \leq y_{c,s,t}, \forall c \in C, t \in T \backslash \{TL\}, s' \in S_c, s \in TO_{c,s'}, cost\,Tr_{c,s,s'} \neq 0 \quad (33)$$

$$x_{c,s,s',t+1} \leq y_{c,s',t+1}, \forall c \in C, t \in T \backslash \{TL\}, s' \in S_c, s \in TO_{c,s'}, cost\,Tr_{c,s,s'} \neq 0 \quad (34)$$

Although $x_{c,s,s',t}$ is a continuous variable, restricted by (31)-(34), it is naturally enforced to be 1 when both $y_{c,s,t}$ and $y_{c,s',t+1}$ equal to 1; otherwise it equals to zero.

The final MILP model with a tighter LP relaxation is given by (1)-(16), (18)-(26), (28)-(29) and (31)-(34).

7. Alternative formulations

To demonstrate its efficiency, the proposed APSTN based model is compared with two alternative MILP models: the precedence-based (PB) model and the original PSTN model. The formulations of the alternative models,

consistent with the nomenclature from section 5, are presented as follows. It is noted that both alternative models share the same production related constraints, which are the ones in section 5.1 to section 5.5. The main difference of the formulations lies in the way to represent the transition of operating states, reflected in the constraints described from section 5.6.

7.1 Precedence-based formulation

As for the PB formulation, we refer to the state transition and minimum operating time constraints ((12), (13) and (15)) of the model in Mitra *et al.*[4], which addresses the scheduling problem of continuous processes including air separation production. The state transition constraints, (12) and (13) in Mitra *et al.*[4], are then reformulated as constraint (15) in Mitra *et al.*[12], where the two constraints are aggregated into one constraint, and number of constraints is consequently reduced. The formulations from Mitra *et al.*[4] and the improved reformulation in Mitra *et al.*[12] are shown to be efficient and are adopted in other works, such as Zhang *et al.*[5-6]. With the nomenclature in this paper, the constraints are rewritten as (35) and (36), which represent the transitions and minimum operating time, respectively. The objective function for the PB model is reformulated as (37), where $z_{c,s,s',t}$ is a binary variable, which equals to 1 if unit *c* is operated with state *s* during time *t*-1 and state *s'* during time *t*; To_s is the set of operating states that from which state s can be directly reached; and $From_s$ is the set of operating states that state s can directly transfer to. It is important to note that the binary variable that accounts for transitions has associated one more index (*s'*), which increases the total number of binary variables of the model.

$$\sum_{s' \in To_s} z_{c,s',s,t} - \sum_{s' \in From_s} z_{c,s,s',t} = y_{c,s,t} - y_{c,s,t-1}, \forall c \in C, s \in S_c, t \in T \backslash \{1\} \tag{35}$$

$$y_{c,s',t} \geq \sum_{\theta=0}^{ms_{s'}-1} z_{c,s,s',t-\theta}, \forall c \in C, s \in S_c, t \in T \tag{36}$$

$$TC = \sum_{c \in C} \sum_{t \in T} wp_t \cdot P_{c,t} + \sum_{c \in C} \sum_{s \in S_c} \sum_{s' \in From_s} \sum_{t \in T} cost\ EP_t \cdot p_{c,s,s'} \cdot z_{c,s,s',t} + \sum_{t \in T} cost\ QBK \cdot QBK_t \tag{37}$$

7.2 PSTN formulation

The formulations in Basán *et al.*[7] describe the scheduling of an air separation process of one unit under the PSTN framework. Each of the operating state is decomposed into three sub-states: initial state s_i, intermediate state s_{n-1} and final state s_n, respectively. The transitions between operating states and the requirement of minimum operating time are represented by logic-based constraints. It has to be noted that we consider a transition network that comprises different operating states from the ones in Basán *et al.*[7]. Therefore, only the constraints that are applicable to our problem, which are (1)-(3), (6)-(8) and (9)-(10) in their paper are adopted here as the alternative formulations. With the notations in this paper, the PSTN formulation is rewritten as follows. Some new sets of sub-states corresponding to unit *c* are included in the formulations, which are the set of initial sub-state $InitS_c$, the set of intermediate sub-state $InterS_c$, and the set of final sub-state $FinalS_c$. S_c^{all} is the set of all possible operating states for unit *c*. Constraint (38), which corresponds to equation (1) in Basán *et al.*[7], represents only one operating state that is running for each unit *c* and time period *t*. (39)-(41) and (42) correspond to the constraints representing sequential transitions ((2)-(3), (6)-(8) in Basán *et al.*[7]) and critical transition ((9) in Basán *et al.*[7]) of operating state, respectively. (43) is the minimum operating time constraint.

$$\sum_{s \in S_c^{all}} y_{c,s,t} = 1, \forall c \in C, t \in T \tag{38}$$

$$y_{c,s,t} = y_{c,s',t+1}, \forall c \in C, s \in InitS_c, s' \in InterS_c, t \in T \backslash \{TL\} \tag{39}$$

$$y_{c,s,t} \leq y_{c,s',t+1}, \forall c \in C, s \in InterS_c, s' \in FinalS_c, t \in T \backslash \{TL\} \tag{40}$$

$$y_{c,s,t+1} \leq \sum_{s' \in To_s} y_{c,s',t}, \forall c \in C, s \in InitS_c, t \in T \backslash \{TL\} \tag{41}$$

$$y_{c,s,t} \leq \sum_{s' \in From_s} y_{c,s',t+1}, \forall c \in C, s \in FinalS_c, t \in T \backslash \{TL\} \tag{42}$$

$$(ms_s - 2) \cdot y_{c,s,t} \leq \sum_{t'=t+1}^{t+ms_s-2} y_{c,s',t'}, \forall c \in C, s \in InterS_c, s' \in FinalS_c, t \in T, t \leq TL - (ms_s - 2) \tag{43}$$

8. Case study and numerical experiments

For the case study in this paper, we consider an air separation process. The site under study has two heterogeneous parallel cold boxes as shown in Fig. 4. Unit 1 has one MAC and BAC, and one cold box, while Unit

2 has an extra expansion turbine to reduce the temperature of reflux stream. In addition, only Unit 1 produces liquid argon (LAR).

The associated information of each operating state, such as the correlation coefficient of production level between products, the maximum and minimum production levels, are obtained from historical production data, and is considered as a model input. The discretized operating states considered in the case study are described in Table 1. The information related to transition costs and minimum operating time of the different states is shown in Fig. 5.

All instances were implemented in GAMS 24.9.2 and solved with CPLEX 12.7.1.0 with default options. The relative optimality tolerance is set to zero. Instances in section 8.1 to section 8.3 are all based on real production data. For the instances in the sensitivity analysis in section 8.4, all the data is based on real production data except the data of product demand, which is generated based on nominal value (real production data). The hardware consisted on a laptop with Intel i7-7500U (2.70GHz) with 16G RAM running with Windows 10 system, and one thread is used by CPLEX solver.

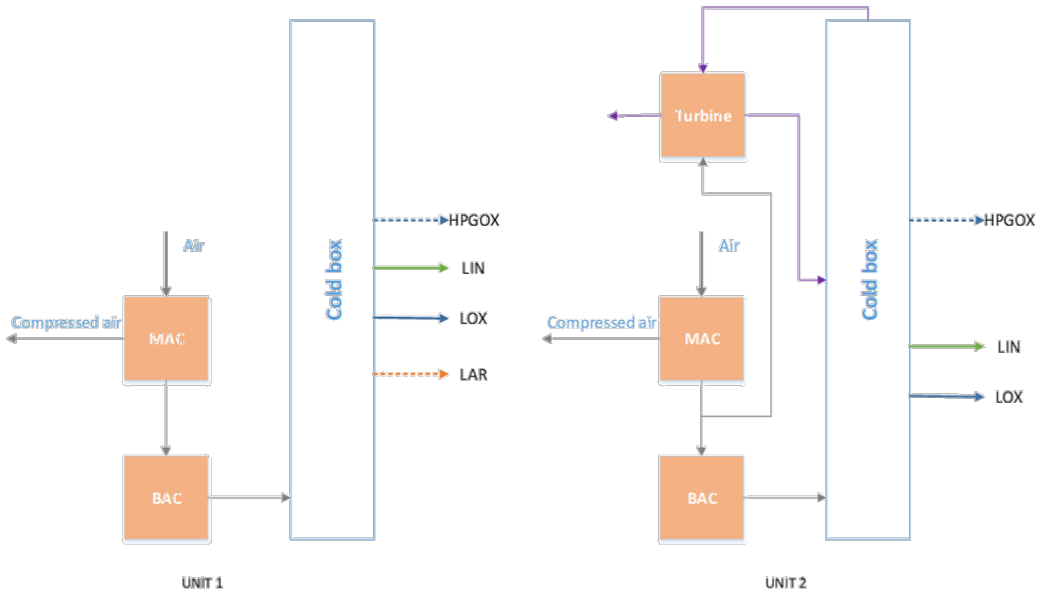

Figure 4. Units' configuration. MAC and BAC stand for main air compressor and booster air compressor, respectively.

Table 1. Production state description.

Unit	State	Equipment	Liquid Production						Gaseous Production			
			LIN		LOX		LAR		HPGOX		CA	
			min	max	min	max	min	max	min	max	min	max
1	Shut-down (S1)	-	-	-	-	-	-	-	-	-	-	-
	No LIN Production (S2)	MAC	-	-	✓	✓	0	✓	✓	✓		✓
	LIN Production (S3)	MAC	✓	✓	✓	✓	0	✓	✓	✓		✓
2	Shut-down (S4)	-	-		-	-	-	-	-	-	-	-
	Low Air production level (S5)	MAC	0	✓	✓	✓	-	-	✓	✓		✓
	High Air production level (S6)	MAC Turbine	0	✓	✓	✓	-	-	✓	✓		✓

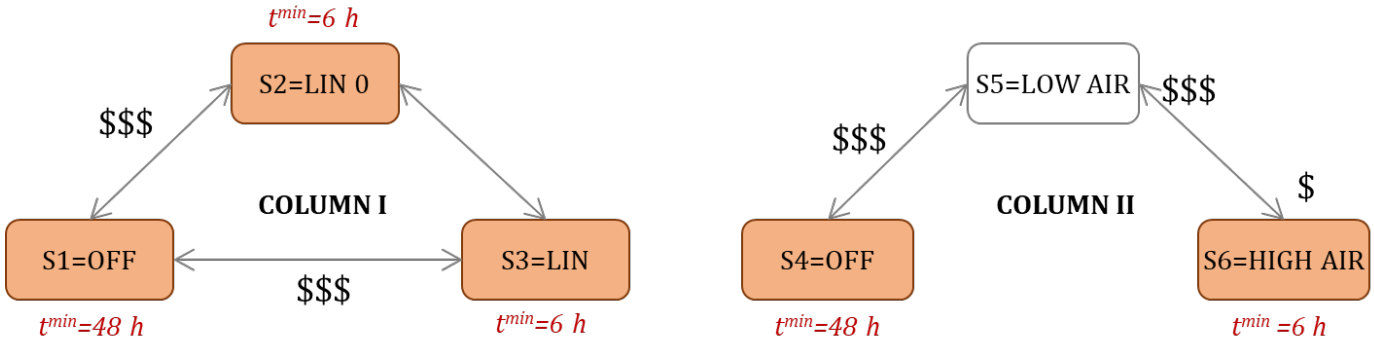

Figure 5. Operation states and allowed transitions within the different units.

8.1 Nominal case

The model is tested for a scheduling time horizon of one week on an hourly basis. The profile of the electricity price forecast is presented in Fig. 6. There is a continuous demand of the gaseous product HPGOX and compressed air, whereas the liquid production demands occur every 12 hours, as shown in Fig. 7. The operating states in this case are listed in Table 1. The minimum operating time of S1 to S6 is {48, 6, 6, 48, 0, 6} hours, respectively. The optimal production levels, inflow air and compressed air production level are shown in Fig. 8, Fig. 9, Fig. 10 and Fig. 11. We can see from the figures that the production levels are varying with the electricity price. For the periods with higher price, the air inflow is adjusted to a relative lower level to minimize the electricity costs. However, the production is also subject to demand and inventory requirements.

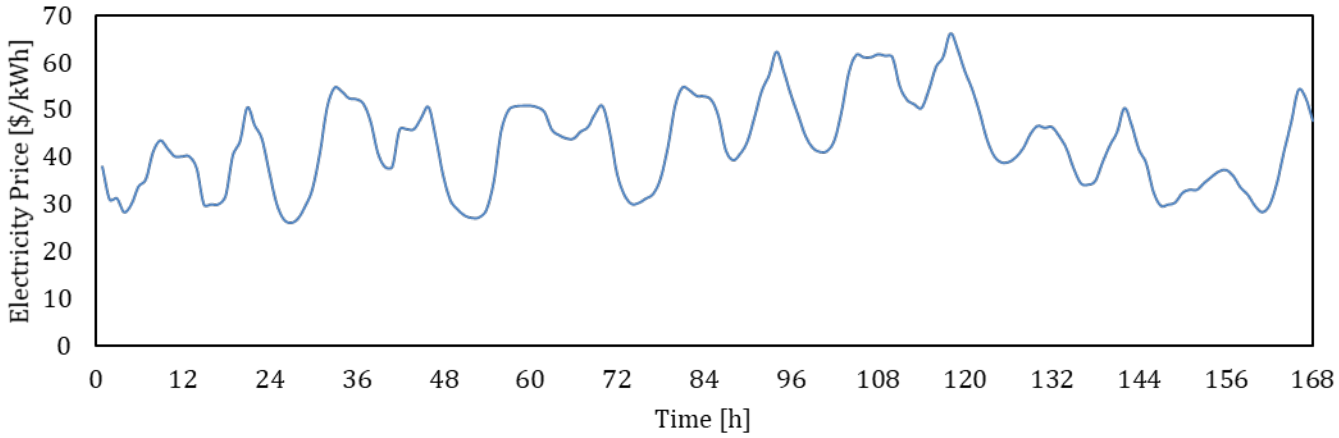

Figure 6. Electricity price forecast.

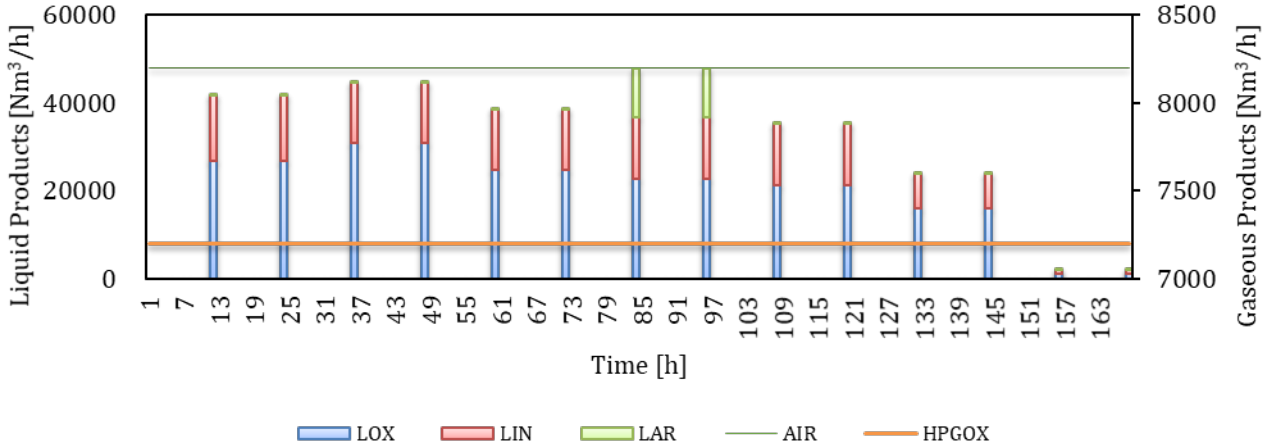

Figure 7. Liquid and gaseous product demand.

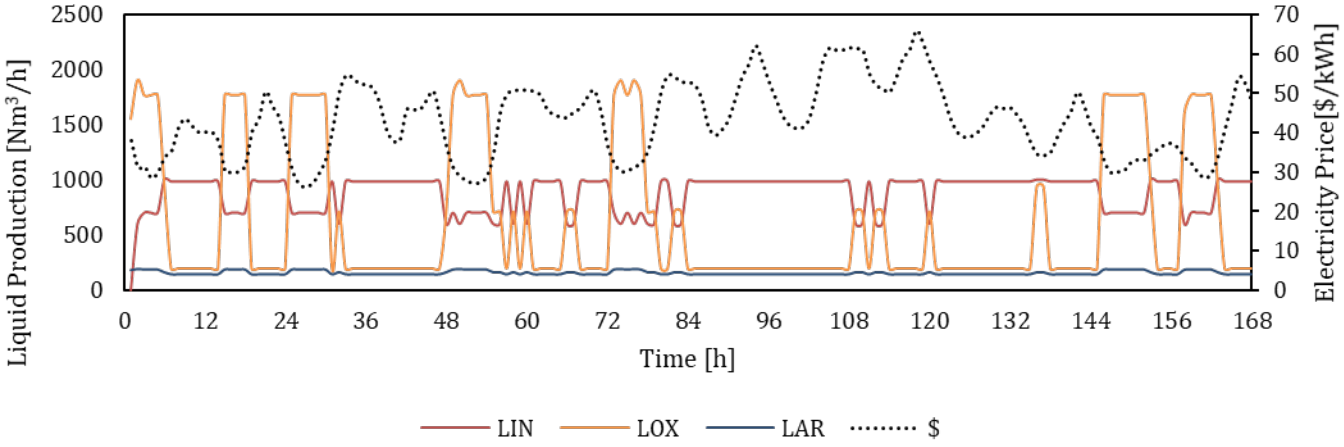

Figure 8. Liquid Production in unit 1.

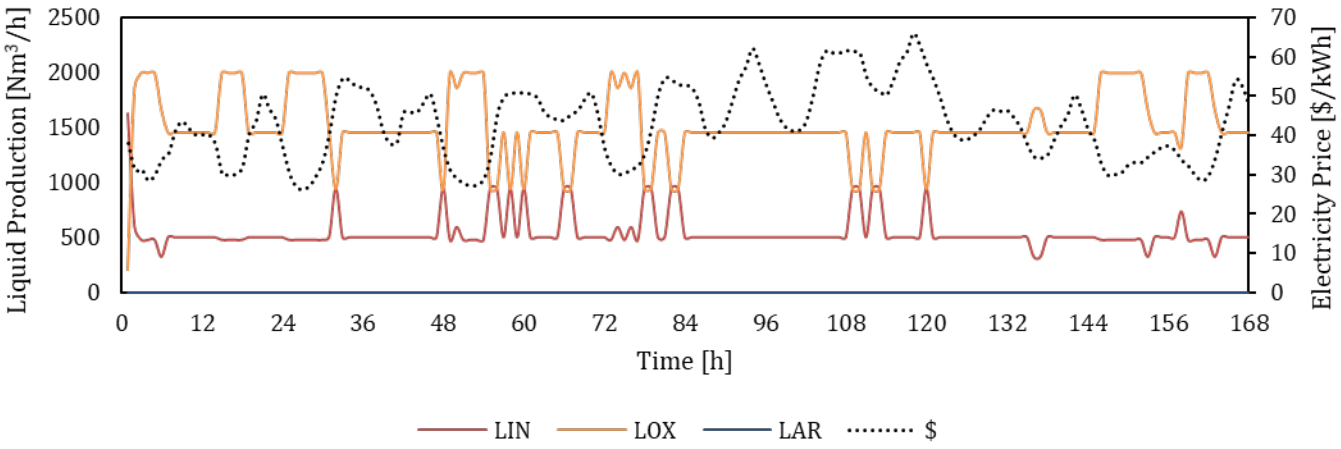

Figure 9. Liquid Production in unit 2.

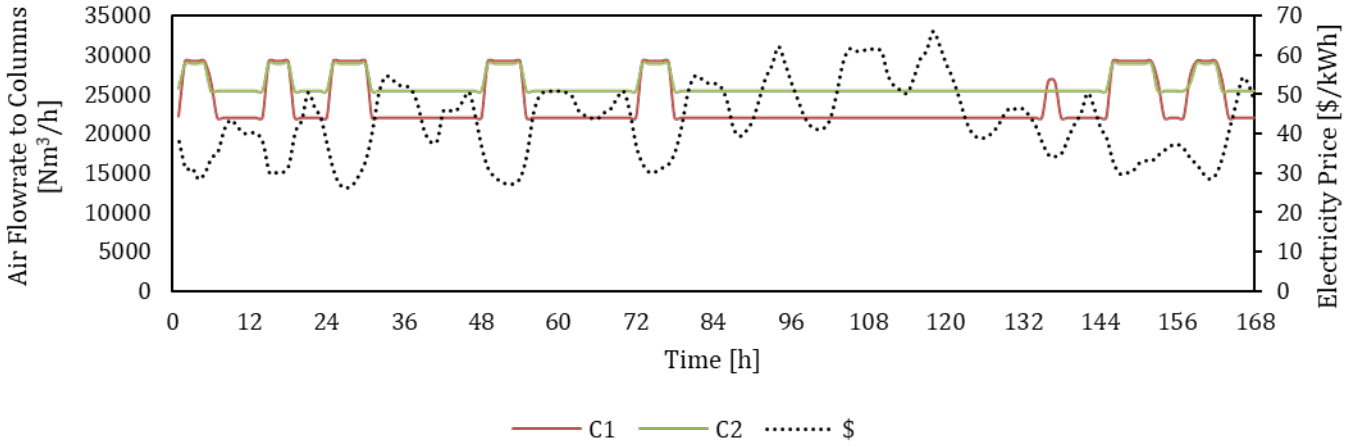

Figure 10. Air Flowrate to columns.

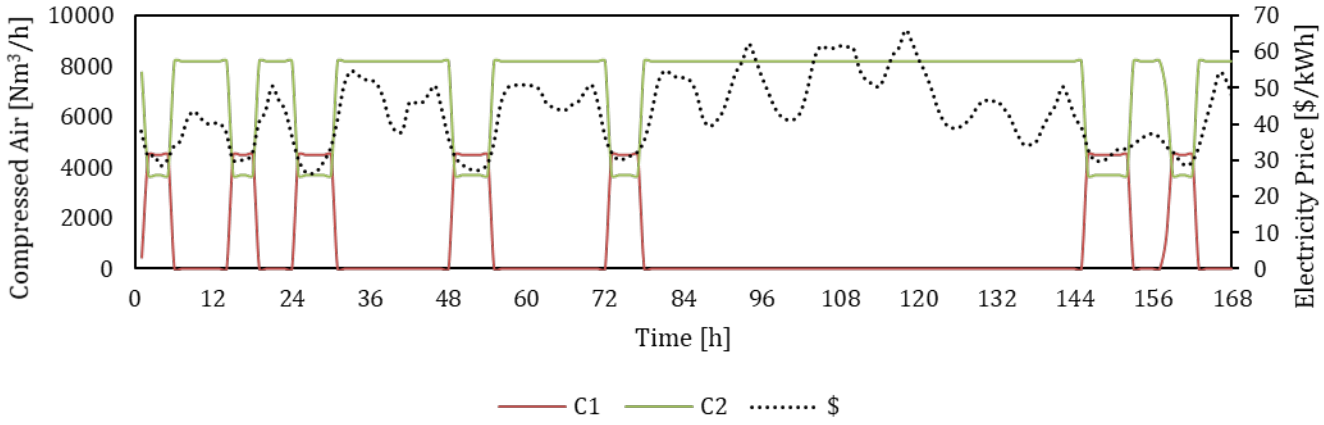

Figure 11. Compressed Air production level

8.2 Model performance with variable number of disaggregated states

First, we analyze the influence of the number of states with minimum operating time on the computational performance on the PB, PSTN and APSTN models considering two different instances. Instance 1# consists of three states with minimum operating time, whereas instance #2 consists of five states with minimum operating time (see Table 2). For example, the minimum operating time of state S1 and S2 within the two instances are 0 hour and 6 hours, respectively. The time horizon for both instances is 1 week with one-hour length time intervals.

As it can be seen in Table 2, for Instance #1, all the three models are able to obtain the optimal solutions in short times, where APSTN requires the shortest time. Regarding the LP relaxation, the PB model is slightly tighter than the APSTN model and much tighter than the PSTN model. However, the number of binary variables of the APSTN model is 44% less than the PB model. While for Instance #2 where 5 out of 6 operation states have minimum operating time, the PSTN model cannot obtain the optimal solution within one hour of computational time. The reason for why PSTN is not that efficient with the transition network in this paper can be explained as follows. Compared to the transition network in this paper, the one in which the PSTN model performs efficiently in Basán *et al.*[7], has the feature that the sequence of the state transitions is relatively constrained. Therefore, for the PSTN model, the decision space is reduced compared to the one in this paper. Moreover, the transition network in this paper accounts for more states with minimum operating time that need to be disaggregated, which significantly increases the number of binary variables and constraints, and consequently increases the difficulty of solving the model. The PB and APSTN models obtain the optimal solution in rather short solution times. It is important to note that the APSTN obtains the optimal solution at the root node for both Instance #1 and #2, and also PSTN obtains optimal solution for Instance #1 at the root node. This can be explained by the pre-solve processing performed by CPLEX, where cutting planes are added at the root before the branching, regarding to the underlying logic constraints of the APSTN model, and PSTN as well.

Table 2. Computational results of instances with variable minimum operating time.

Formulation	Instance	Minimum operating time for states (hour)						Model size			Cost	LP relaxation gap	# of Nodes	Optimality Gap (%)	CPUs
		S1	S2	S3	S4	S5	S6	# bin. vars.	# cont. vars.	# constraints					
PB Precedence based	#1	48	0	0	48	0	6	2,684	5,546	21,004	31,089,230	10.7%	480	-	6.19
	#2	48	6	6	48	0	6	2,684	5,546	21,676	31,089,230	10.7%	2,013	-	8.52
PSTN	#1	48	0	0	48	0	6	2,014	6,548	41,366	31,089,230	23.5%	0	-	2.20
	#2	48	6	6	48	0	6	2,686	7,220	56,802	31,089,230	-	105,893	2.8%	3,600
APSTN	#1	48	0	0	48	0	6	1,507	6,044	26,686	31,089,230	11.7%	0	-	1.88
	#2	48	6	6	48	0	6	1,841	6,380	28,360	31,089,230	11.7%	0	-	2.94

LP relaxation gap: (MIP – LP relaxation)/MIP. Optimality gap: (Upper Bound - Lower Bound)/Upper Bound.

8.3 Model performance regarding to variable length of time interval

In order to analyze the efficiency of the models, we also test the models on instances with different combination of scheduling time horizons and sizes of time intervals, which are instances #3 to #6 in Table 3. For these instances, the number of disaggregated operation states is set to be the same as the Instance #2 in Section 8.2. For instance #4, who has half hour time intervals, the first half and the second half of each hour has the same electricity price, and the price is equal to the hourly price in instance #5 for the same hour. While for instance #3, another setting of electricity prices is used. We introduce some variation between the quarterly electricity prices in one hour to verify that the production levels are adjusted accordingly. The computational results are listed in Table 3.

In this section, only PB and APSTN models are analyzed. As shown in Table 3, the LP relaxation of the PB model is also slightly tighter than the APSTN model, while the number of binary variables is reduced by more than 30%. For every instance, the APSTN model can obtain the optimal solution with shorter solution time than the PB model. Especially for Instance #6, where a two-week time horizon and one hour of time interval length is considered, the solution time is significantly reduced. It is noted that for Instances #4 to #6, the optimal solutions are obtained at the root node. From instance #4 to instance #5, we can see that the objective function is improved as the time grids get smaller.

Table 3. Computational results with various sizes of time intervals.

Formulation	Instance	Time horizon	Time interval	Model size			Cost	LP relaxation gap	# of Nodes	CPUs
				# bin. vars.	# cont. vars.	# constraints				
PB Precedence-based	#3	1 week	0.25h	10,748	22,178	86,692	32,089,462	10.7%	612	151.41
	#4	1 week	0.5h	5,372	11,090	43,348	31,089,044	10.8%	522	17.16
	#5	1week	1h	2,684	5,546	21,676	31,089,230	10.7%	2013	8.52
	#6	2week	1h	5,372	11,090	43,348	62,281,349	12.1%	5211	195.06
APSTN	#3	1 week	0.25h	7,385	25,532	113,536	32,089,462	11.7%	570	146.05
	#4	1 week	0.5h	3,689	12,764	56,752	31,089,044	11.7%	0	8.50
	#5	1week	1h	1,841	6,380	28,360	31,089,230	11.7%	0	2.94
	#6	2week	1h	3,689	12,764	56,752	62,281,349	13.0%	0	18.78

8.4 Sensitivity Analysis

Considering Instance #6, with a two-week time horizon and time interval of one hour, we perform optimizations of production scheduling with the PB and APSTN formulations for different values of product demands. We generate 1000 scenarios of demand normally distributed around the nominal demand profile with a standard deviation of 10%.

Not all the scenarios can be solved to optimality within 600 s for both formulations. 75.4% and 70.6% of the scenarios are solved to optimality in the case of the APSTN and PB, respectively. Considering only these scenarios, it is important to note that 29% of them are solved at the root node for the APSTN, whereas 15% in the case of the PB formulation. Finally, the average CPU for the APSTN is 52 s, shorter than the PB, which is 143 s.

9. Conclusion

In this paper, a scheduling problem of air separation production has been addressed. The goal of the scheduling problem is to minimize the total production cost under variable day ahead electricity price by properly adjusting the operating state of the units and consequentially adjusting the production levels. To represent the transition network

of air separation process, the APSTN framework is developed which is efficient for the network that has many potential transitions. The APSTN is a generalized framework that can be applied to other industrial process with state transitions. Applying APSTN, a tight discrete time MILP model is developed to address the scheduling problem. The model has been tested on different instances with industrial data and demonstrated to be efficient. The APSTN framework and the tight MILP model provide a solid basis for the potential research on energy intensive processes under uncertainty, e.g. flexibility analysis on the scheduling of air separation process.

Acknowledgements

The authors gratefully acknowledge the financial support from National Key Research and Development Program of China (2016YFB0901900), the Fund for Innovative Research Groups of the National Natural Science Foundation of China (71621061), the Major International Joint Research Project of the National Natural Science Foundation of China (71520107004), the Major Program of the National Natural Science Foundation of China (71790614), the 111 Project (B16009), the Center for Advanced Process Decision-making at Carnegie Mellon University and the China Scholarship Council.

References

1. Zhang, Q.; Grossmann, I. E. Enterprise-wide Optimization for Industrial Demand Side Management: Fundamentals, Advances, and Perspectives. *Chem. Eng. Res. Des.* **2016**a, 116, 114-131..
2. Hadera, H.: Harjunkoski, I.; Sand, G.; Grossmann, I. E.; Engell, S. Optimization of steel production scheduling with complex time-sensitive electricity cost. *Comput. Chem. Eng.* **2015**, 76, 117–136.
3. Castro, P.; Sun, L.; Harjunkoski, I. Resource–task network formulations for industrial demand side management of a steel plant. *Ind. Eng. Chem. Res.* **2013**, 52(36), 13046–13058.
4. Mitra, S.; Grossmann, I. E.; Pinto, J. M.; Arora, N. Optimal Production Planning Under Time-sensitive Electricity Prices for Continuous Power-Intensive Processes. *Comput. Chem. Eng.* **2012**, 38, 171.
5. Zhang, Q.; Sundaramoorthy, A.; Grossmann, I. E.; Pinto, J. M. A discrete-time Scheduling Model for Continuous Power-intensive Process Networks with Various Power Contracts. *Comput. Chem. Eng*. **2016**b, 84, 382.
6. Zhang, Q.; Cremer, J. L.; Grossmann, I. E.; Sundaramoorthy, A.; Pinto, J. M. Risk-based Integrated Production Scheduling and Electricity Procurement for Continuous Power-intensive Processes. *Comput. Chem. Eng*. **2016**c, 86, 90.
7. Basán, N. P.; Grossmann, I. E.; Gopalakrishnan, A.; Lotero, I.; Medez, C. A. Novel MILP Scheduling Model for Power-Intensive Processes under Time-Sensitive Electricity Prices. *Ind. Eng. Chem. Res.* **2018**, 57(5): 1581–1592.

8. Floudas, C.; Lin, X. Continuous-time versus discrete time approaches for scheduling of chemical processes: a review. *Comput. Chem. Eng.* **2004**, 28(11), 2109-2129.

9. Méndez, C. A.; Cerdá, J.; Grossmann, I. E.; Harjunkoski, I.; Fahl, M. State-of-the-art Review of Optimization Methods for Short-term Scheduling of Batch Processes. *Comput. Chem. Eng.* **2006**, 30 (6−7), 913.

10. Maravelias, C. General framework and modeling approach classification for chemical production scheduling. *AIChE J.* **2012**, 58(6), 1812-1828.

11. Harjunkoski, I.; Maravelias, C. T.; Bongers, P.; Castro, P. M.; Engell, S.; Grossmann, I. E.; Hooker, J.; Méndez, C.; Wassick, J. Scope for Industrial Applications of Production Scheduling Models and Solution Methods. *Comput. Chem. Eng.* **2014**, 62, 161.

12. Mitra, S.; Sun, L.; Grossmann, I. E. Optimal Scheduling of Industrial Combined Heat and Power Plants Under Time-sensitive Electricity Prices. *Energy* **2013**, 54, 194.

13. Zhang, Q.; Bremen, A. M.; Grossmann, I.E.; Pinto, J.M. Long-Term Electricity Procurement for Large Industrial Consumers under Uncertainty. *Ind. Eng. Chem. Res.* **2018**, 57 (9), 3333-3347.

14. Castro, P.; Harjunkoski, I.; Grossmann, I.E. New continuous-time scheduling formulation for continuous plants under variable electricity cost. *Ind. Eng. Chem. Res.* **2009**, 48(14), 6701–6714.

15. Castro, P.; Harjunkoski, I.; Grossmann, I.E. Optimal scheduling of continuous plants with energy constraints. *Comput. Chem. Eng.* **2011**, 35(2), 372–387.

16. Zhang, X.; Hug, G.; Harjunkoski, I. Cost-effective scheduling of steel plants with flexible EAFs. IEEE Trans. Smart Grid **2017**, 8, 239–249.

17. Cao, Y.; Swartz, C. L. E.; Baldea, M. Design for dynamic performance: Application to an air separation unit. *Am. Control Conf.* **2011**, 2683−2688.

18. Cao, Y.; Swartz, C. L. E.; Baldea, M.; Blouin, S. Optimization based assessment of design limitations to air separation plant agility in demand response scenarios. *J. Process Control* **2015**, 33, 37−48.

19. Cao, Y.; Swartz, C. L. E.; Flores-Cerrillo, J.; Ma, J. Dynamic modeling and collocation-based model reduction of cryogenic air separation units. *AIChE J.* **2016**, 62(5):1602-1615.

20. Pattison, R.C.; Touretzky, C.R.; Johansson, T.; Harjunkoski, I.; Baldea, M. Optimal process operations in fast-changing electricity markets: framework for scheduling with low-order dynamic models and an air separation application. *Ind. Eng. Chem. Res.* **2016**, 55, 4562–4584.

21. Dias, S.; Pattison, R. C.; Tsay, C.; Baldea, M.; Ierapetritou, M. G. A simulation-based optimization framework for integrating scheduling and model predictive control, and its application to air separation units. *Comput. Chem. Eng.* **2018**, 113, 139–151.

22. Nolde, K.; Morari, M. Electrical load tracking scheduling of a steel plant. *Comput. Chem. Eng.* **2010**, 34(11), 1899–1903.

23. Hait, A.; Artigues, C. On electrical load tracking scheduling for a steel plant. *Comput. Chem. Eng*. **2011**, 12(14), 3044–3047.

24. Hadera, H.; Labrik, R.; Sand, G.; Engell, S.; Harjunkoski, I. An Improved Energy-Awareness Formulation for General Precedence Continuous-Time Scheduling Models. *Ind. Eng. Chem. Res*. **2016**, 55, 1336−1346.

25. Castro, P.; Grossmann, I.E.; Veldhuizen, P.; Esplin, D. Optimal maintenance scheduling of a gas engine power plant using generalized disjunctive programming. *AIChE J.* **2014**, 60, 2083–2097.

26. Zhao, S.; Grossmann, I. E.; Tang L. Integrate d scheduling of rolling sector in steel production with consideration of energy consumption under time-of-use electricity prices. *Comput. Chem. Eng*. **2018**, 111, 55–65.

27. Castro, P.; Grossmann, I.E.; Zhang, Q. Expanding scope and computational challenges in process scheduling. *Comput. Chem. Eng*. **2018**, 114, 14-42.

28. Glover, F. Improved linear integer programming formulations of nonlinear integer programs. *Management Sci*. **1975**, 22, 455-460